



“PHOTOELECTROCHEMICAL BEHAVIOR OF INDIUM SULPHIDE THIN FILMS”

C. Jeyanthi* M. Anithalakshmi**

*Department of Physics, Govt. Arts College, Dharmapuri.

**Department of Physics, Adhiyaman Arts and Science College for Women, Uthangarai, Krishnagiri.

Abstract

In₂S₃ films were deposited by the pulse electro deposition technique on tin oxide coated glass substrates, at different duty cycles in the range of 6% - 50%. The deposition potential was -0.4 V Vs saturated calomel Electrode (SCE) using 0.1 M of InCl₃ and 0.02 M of Sodium thiosulphate in di-ethylene glycol. XRD analysis of the films indicated polycrystalline tetragonal nature. Grain size, strain and dislocation density were evaluated from the XRD data, EDX analysis of the surface composition confirms the formation of stoichiometric In₂S₃ films. The binding energies of In and S are confirmed from XPS studies. The surface morphological studies for grown In₂S₃ film for different duty cycle is observed from AFM analysis. The Raman spectra of grown In₂S₃ for different duty cycles indicated that the width of peak decreases with increase of duty cycles. Optical studies show a direct band gap values in the range of 2.18 – 2.04 eV for the films deposited at different duty cycles. Room temperature resistivities of the grown films were in the decreasing range from 10⁶ Ωcm to 10³ Ωcm with the increase of duty cycle. Photoelectrochemical (PEC) constructed with the films deposited at 50% duty cycle and post heated at 500°C indicated open circuit voltage (V_{oc}) of 0.48V, Short circuit current density (J_{sc}) of 5.80 mAcm², fill factor (ff) of 0.68, efficiency (η) of 3.13%, Series resistance (R_s) of 4Ω and shunt resistance (R_{sh}) of 2.6Ω making use of the advantages of pulse electro deposition it can be used to deposit nanocrystalline films which can be employed in optoelectronic and photovoltaic devices.

KeyWords:Thin Film, Saturated Calomel Electrode, Sodium Thiosulphate, Stoichiometric, Photoelectrochemical, Nanocrystalline, Optoelectronic And Photovoltaic Devices.

1. Introduction

Indium sulfide is a non-toxic material and is an n-type semiconductor with an energy band gap of 2.5 eV, and has been used efficiently as a photoconducting material [7,8]. In₂S₃ is a III–VI compound and it crystallizes in tetragonal structure with the lattice parameters, a = 7.619 Å and c = 32.329 Å. It exists in three forms such as α, β and γ depending on the growth temperature and pressure [1]. Among these three forms, β -In₂S₃ is the most stable structure at room temperature. In₂S₃ finds many applications in the preparation of green and red phosphors and in the manufacture of picture tubes for color television [2] and dry cells [3]. It is a promising candidate for many technological applications due to its stability, its interesting structural characteristics and optical properties [4]. In this work, the pulse electrodeposition technique has been employed for the first time to deposit In₂S₃ films. In this chapter, results obtained on In₂S₃ films are presented and discussed.

2. Deposition of Films

In₂S₃ films were deposited by the pulse electro deposition technique at different duty cycles in the range of 6 – 50 %. The deposition potential was – 0.4 V (SCE). The deposition was done at room temperature and the precursors were 0.1 M InCl₃ and 0.02 M sodium thiosulphate in di-ethylene glycol. The total deposition time was maintained as 60 min for all the duty cycles. Thickness of the films measured by surface profilometer was in the range of 400 nm – 700 nm for the films deposited at different duty cycles.

3. Structural Properties of In₂S₃ Films

X-Ray diffraction patterns of the films deposited at different duty cycle is shown in Fig: 1. The films exhibit polycrystallinity with peaks corresponding to the tetragonal structure (JCPDS 25 – 0390). The films exhibited preferred orientation in the (108) direction. The intensity of the peaks increased with duty cycle. Crystallite size measured from the XRD data using Scherrer’s equation ($15\epsilon/aD. 7.619 \times 10^{-10}$) was in the range of 50 – 90 nm with increase of duty cycle. The other parameters like strain, dislocation density were estimated using standard relations. The results are given in Table-1.

Table: 1 Micro Structural parameters of In₂S₃ films deposited at different duty cycles.

Duty cycle (%)	crystal size (nm)	strain (x 10 ⁻³)	dislocation density (lines m ⁻²) x 10 ¹⁴
6	32.42	0.757	4.59



9	34.07	0.941	5.43
15	38.76	1.122	5.69
33	47.68	1.453	5.99
50	52.99	1.631	6.09

4. Elemental Analysis by EDAX and XPS

4.1 Edax Analysis

Composition of the films was obtained from energy dispersive X-Ray analysis (EDAX). In L and S K lines were observed in the spectrum. The average ratio of the percentage of In_2S_3 was 2:3 showing that the samples were in good stoichiometric ratio. EDAX spectrum of the films deposited at 50 % duty cycle is shown in Fig: 2.

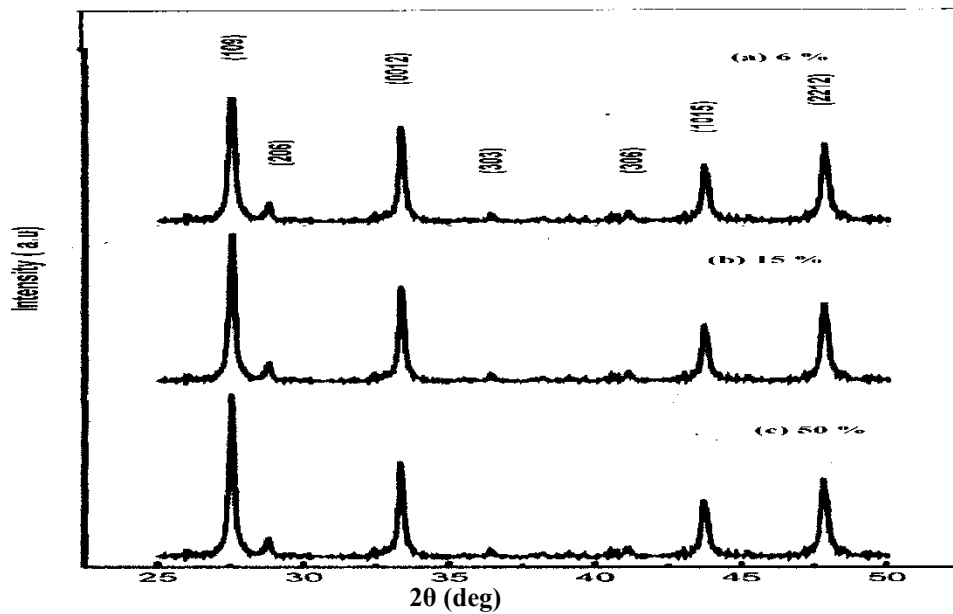


Fig: 1. – X-Ray diffraction pattern of In_2S_3 films deposited at different duty cycles

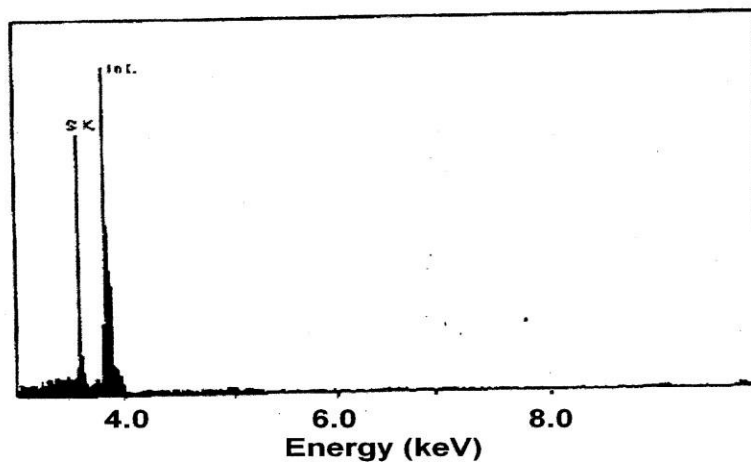


Fig: 2. – EDAX spectrum of In_2S_3 films deposited at 50 % duty cycle



XPS Analysis

Fig: 3. shows the In3d and S2p peaks obtained on the films deposited at different duty cycles. One can see that the binding energies of indium and sulfur do not vary strongly from the films deposited at different duty cycles. The binding energy for S2p is nearly constant at about 162 eV.

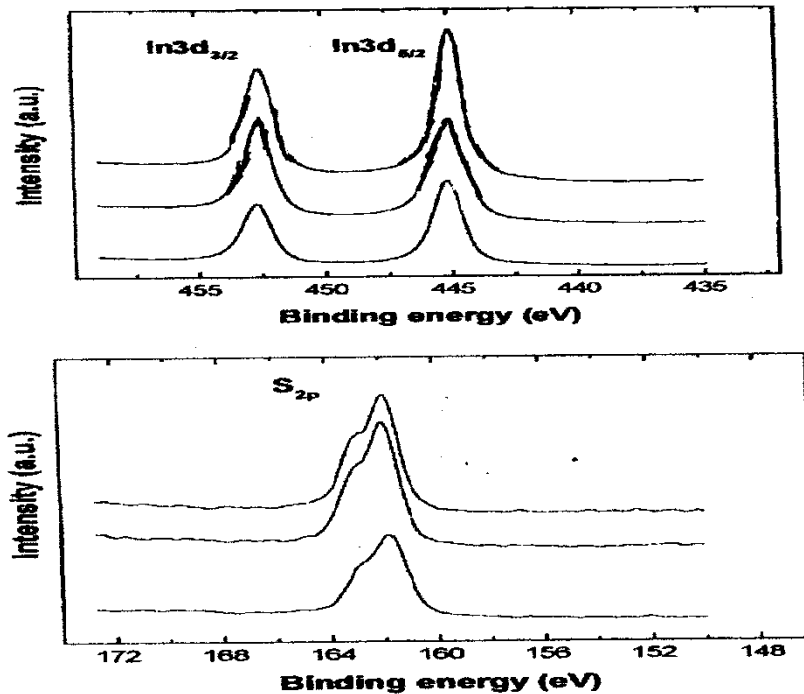
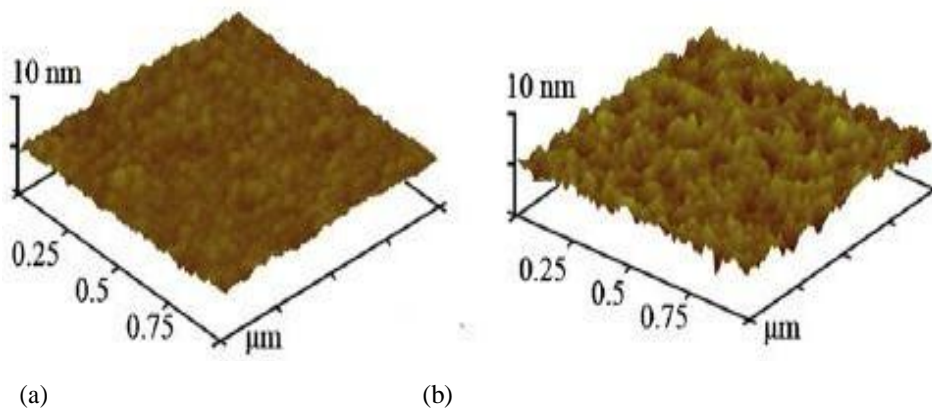


Fig: 3. – XPS spectra of In and S for In_2S_3 films deposited at different duty cycles
(a) 15 % (b) 33 % (c) 50% (Bottom to top)

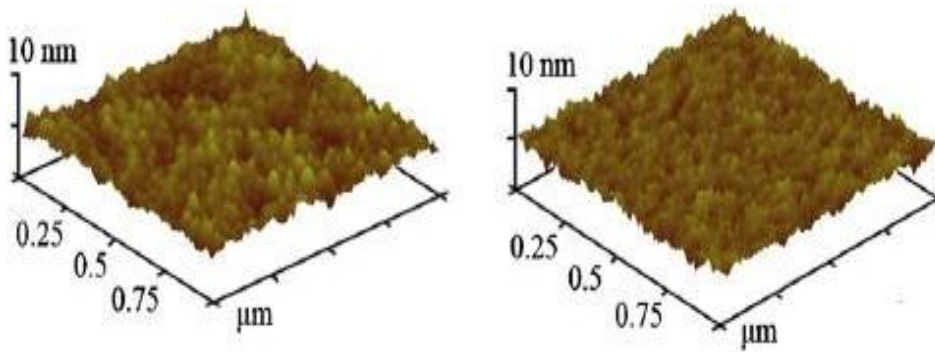
5. Surface Morphological Studies on Deposited Films

The change of surface topography with duty cycle was also analyzed using atomic force microscope (AFM). Fig: 4.(a–d) shows the three-dimensional AFM images of the films deposited at different duty cycles, which clearly indicated the duty cycle - dependent growth of the grains and surface roughness. An increase of the grain size along with an improvement in granularity was observed in In_2S_3 films as the duty cycle was increased. The average grain size of the films varied in the range, 10 – 35 nm with the increase of duty cycle. The retarded grain growth in the layers grown at lower duty cycles might be due the reduced mobility and diffusion of the deposited species on to the substrate surface.



(a)

(b)



(c) (d)
Fig: 4. – Atomic force micrographs of In₂S₃ films deposited at different duty cycles
(a) 6 % (b) 15 % (c) 33 % (d) 50 %

6. Raman Shift Studies of In₂S₃ Films

Room temperature Raman spectra were recorded at room temperature on the In₂S₃ films deposited at different duty cycles. Fig: 5. shows the Raman spectra of In₂S₃ films deposited at different duty cycles. The Raman spectra of grown In₂S₃ are shown in Fig: 5a. for the films deposited at different duty cycles. Raman modes are observed in the energy region between 200 - 500 cm⁻¹, The active modes of β-In₂S₃ are present at 105, 117, 250, 305 and 363 cm⁻¹ [9,10], confirming the composition and structure of the layers. In the present case only the peak at 305 cm⁻¹ and 365 cm⁻¹ were observed, which corresponds to the A1 symmetry. The width of the peak decreases with increase of duty cycle. This is to the increase of grain size with increase of duty cycle.

Room temperature photoluminescence studies did not exhibit any emission characteristics.

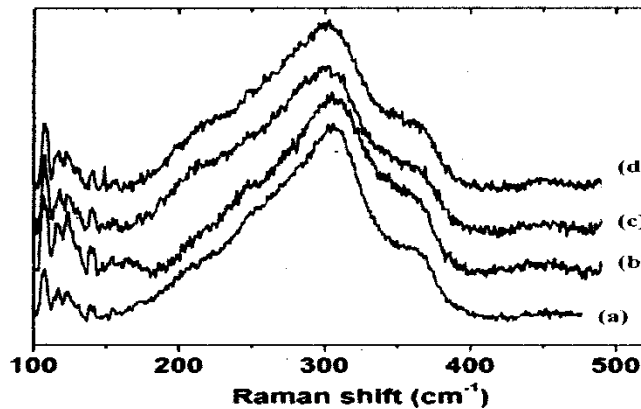


Fig: 5. – Raman spectra of In₂S₃ films deposited at different duty cycles
(a) 50 % (b) 33 % (c) 15 % (d) 6 %

7. Optical Properties of In₂S₃ Films

Fig: 6. shows the transmittance (T), versus wavelength spectrum recorded in the wavelength range, 500–2500 nm for the films deposited at different duty cycles. It can be observed that the measured transmittance of the films at 800 nm, increased from 59.1% to 78% with the increase of duty cycle from 6 % to 50 %. The absorption coefficient, α which is a function of photon energy, $h\nu$ was evaluated by using the relation,

$$\alpha = 1/d \ln (1/T) \dots\dots\dots (1)$$

Where d is the thickness of the film and T is the percentage transmittance.

The optical energy band gap, E_g of the films was determined using the relation,

$$\alpha h\nu = A (h\nu - E_g)^{1/2} \dots\dots\dots (2)$$



Where A is the constant and it is depending on the transition probability. The optical band gap of the films was determined by extrapolating the linear portion of the $(\alpha h\nu)^2$ versus $h\nu$ plot onto the x-axis. Fig. 7. shows the plot for In_2S_3 films deposited at different duty cycles. The evaluated band gap value varied in the range, 2.18–2.04 eV as the duty cycle increased. These values agree with the literature values [5, 6].

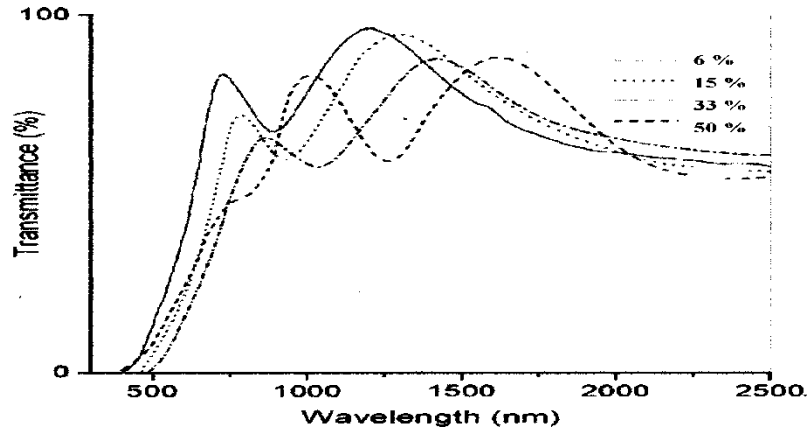


Fig. 6. – Transmission spectra of In_2S_3 films deposited at different duty cycles

The room temperature electrical resistivity of In_2S_3 films was studied as a function of duty cycle using two-probe method. Fig. 8. shows the variation of film resistivity with duty cycle. The resistivity of the films was found to decrease from 10^6 ohm cm to 10^3 ohm cm with increase of duty cycle. The decrease of resistivity with duty cycle is due to the increase of grain size in the films. The present study indicated that the duty cycle had a considerable effect on the electrical properties of the layers. The electrical transport properties are highly sensitive to the density of defects such as dislocations, stacking faults, micro twins, additional phases that are inherent in the growth process of thin films. The defects such as indium interstitials and sulfur vacancies are mainly responsible for the n-type conductivity of the films. Moreover, variation in the size of the grains could also influence the grown layers, the increase of which could decrease the scattering from

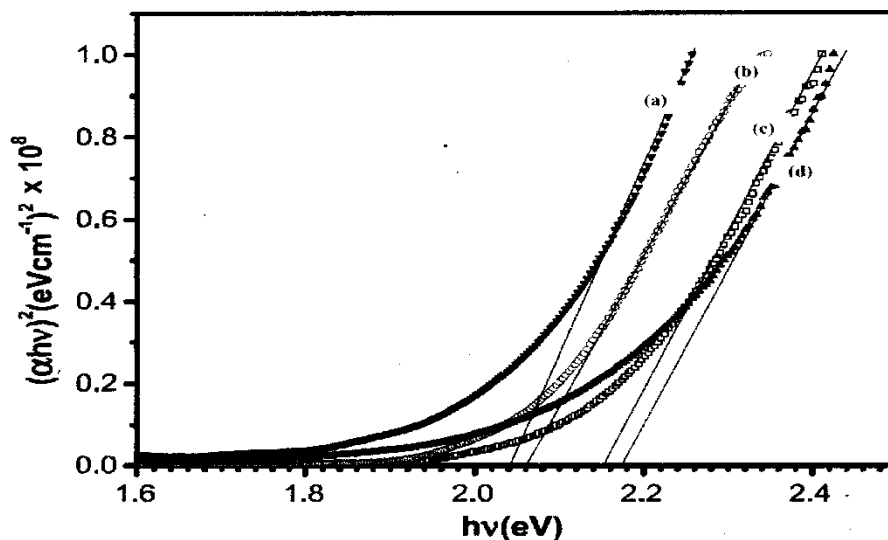


Fig. 7. – $(\alpha h\nu)^2$ versus $h\nu$ plot of In_2S_3 films deposited at different duty cycles
(a) 50 % (b) 33 % (c) 15 % (d) 6 %

the grain boundaries that results in the decrease of electrical resistivity. Hence, the observed lower resistivity for the films deposited at 50 % duty cycle could be due to the well connectivity of the crystallites with improved size in the layers when compared to those prepared at lower duty cycles as observed from the AFM analysis. These resistivity values of In_2S_3 films



observed in the present study are in close agreement with the reported data on the sprayed In_2S_3 films [7]. Due to the high resistivity of the films, mobility and carrier density could not be determined.

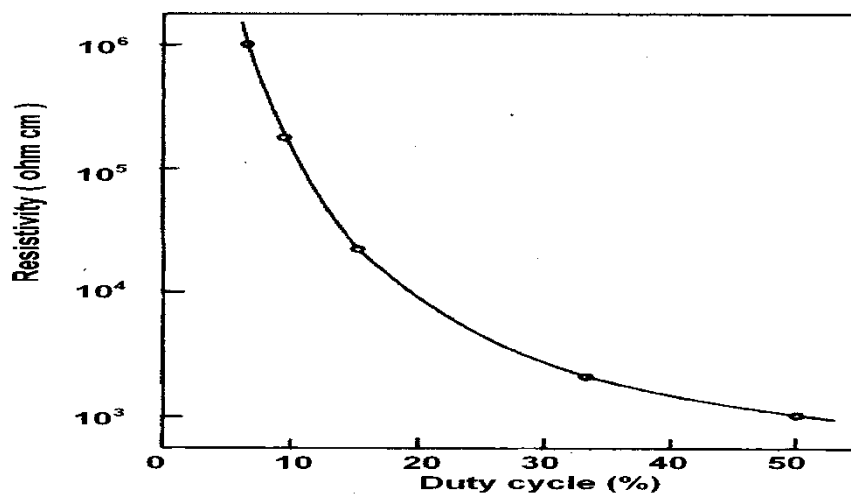


Fig: 8. – Variation of resistivity with duty cycle for In_2S_3 films

8. Photoelectrochemical Studies on In_2S_3 Films

Photoelectrochemical (PEC) cells were prepared using the films deposited on titanium substrates heat treated at different temperatures. The films were lacquered with polystyrene in order to prevent the metal substrate portions from being exposed to the redox electrolyte. These films were used as the working electrode. The electrolyte was 1 M polysulphide. The light source used for illumination was an ORIEL 250 W Tungsten halogen lamp. A water filter was introduced between the light source and the PEC cell to cut off the IR portion. The intensity of illumination was measured with a CEL suryamapi, whose readings are directly calibrated in mWcm^{-2} . The intensity of illumination was varied by changing the distance between the source and the cell. The power output characteristics of the cells were measured by connecting the resistance box and an ammeter in series and the voltage output was measured across the load resistance. The photocurrent, dark current and output voltage were measured with a HIL digital multimeter.

The In_2S_3 photoelectrodes were dipped in the electrolyte and allowed to attain equilibrium under dark conditions for about 10 minutes. The dark current and voltage values were noted. The cells were then illuminated by the light source and the current and voltage were measured for each setting of the resistance box. The photocurrent and photovoltage were calculated as the difference between the current under illumination and the dark current, and voltage under illumination and dark voltage respectively.

PEC formed with the films deposited at different duty cycles did not exhibit any photoactivity. Hence, they were post heat treated in argon atmosphere at different temperatures in the range of 400 - 525°C. The power output characteristics of the PEC cells made using the photoelectrodes deposited at different duty cycles and post heat treated at different temperatures are shown in Fig: 9. – Fig: 13. From the figures, it is observed that the PEC output parameters, viz., open circuit voltage and short circuit current were found to increase for the electrodes heat treated up to a temperature of 500°C. Photoelectrodes heat treated at temperatures greater than this value exhibited lower open circuit voltage and short circuit current due to the reduction in thickness of the films as well as the slight change in stoichiometry. Hence, further studies were made only on the films heat treated at 500°C. The power output characteristics of the electrodes heat treated at 500°C were studied at different intensities of illumination in the range 20-100 mWcm^{-2} . A plot of $\ln J_{sc}$ vs V_{oc} (Fig: 14.) yielded a straight line and the reverse saturation current density J_0 was $2.5 \times 10^{-7} \text{ A cm}^{-2}$. The ideality factor (n) was calculated from the slope of the straight line and it was found to be 1.80.

The effect of photoetching on the PEC performance was studied by shorting the photoelectrode and the graphite counter electrode under an illumination of 100 mWcm^{-2} in 1:100 HCl for different durations in the range 0 – 100 s. Both photocurrent and photovoltage are found to increase up to 60 s photoetch, beyond which they begin to decrease (Fig: 15.). Photoetching leads to selective attack of surface states not accessible to chemical etchants. It is observed that during photoetching, the open



circuit voltage and short circuit current density increase from 4.5 mA cm^{-2} to 5.8 mA cm^{-2} and from 0.43 to 0.48 V respectively for an intensity of 60 mWcm^{-2} . The decrease in the voltage and current beyond 60s photoetching can be attributed to separation of grain boundaries due to prolonged photoetching [8]. The power output characteristics (Fig: 16.) after 60s photoetching indicates a V_{oc} of 0.48 V , J_{sc} of 5.80 mAcm^{-2} , ff of 0.68 and η of 3.13% for 60 mWcm^{-2} illumination. The photovoltaic parameters of the electrodes deposited at different duty cycles and post heat treated at 500°C along with the parameters of the electrodes deposited at 50% duty cycle after post heat treatment with photoetching are shown in Table. 2.

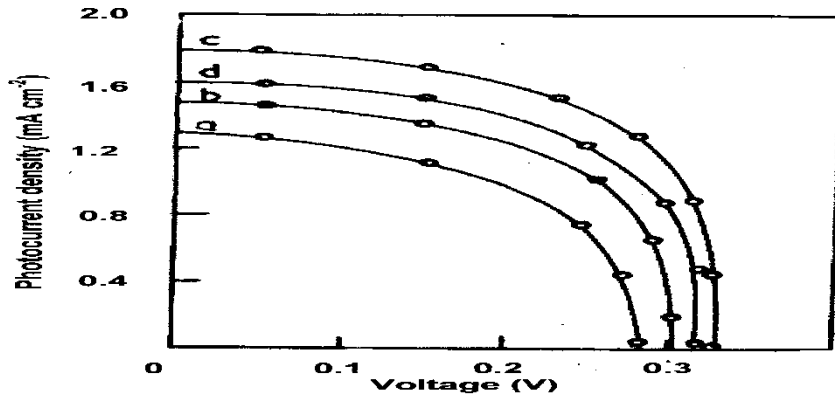


Fig: 9. – Load characteristics of In_2S_3 films deposited at 6 % duty cycles and post heat treated at different temperatures (a) 400°C (b) 450°C (c) 500°C and (d) 525°C

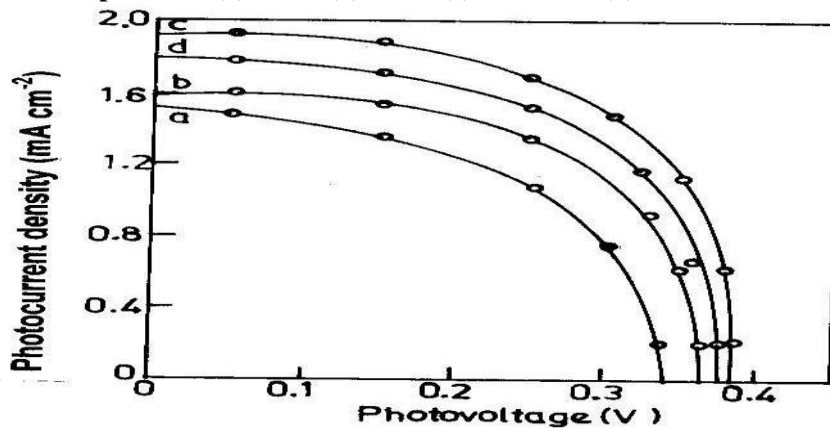


Fig: 10. – Load characteristics of In_2S_3 films deposited at 9 % duty cycles and post heat treated at different temperatures (a) 400°C (b) 450°C (c) 500°C and (d) 525°C

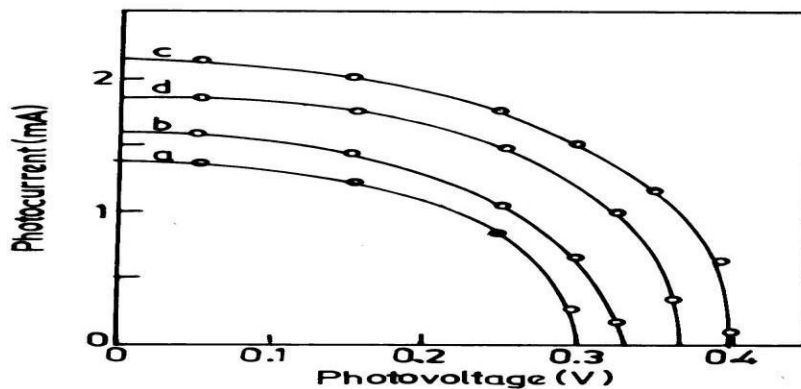




Fig: 11. – Load characteristics of In_2S_3 films deposited at 15 % duty cycles and post heat treated at different temperatures (a) 400°C (b) 450°C (c) 500°C and (d) 525°C

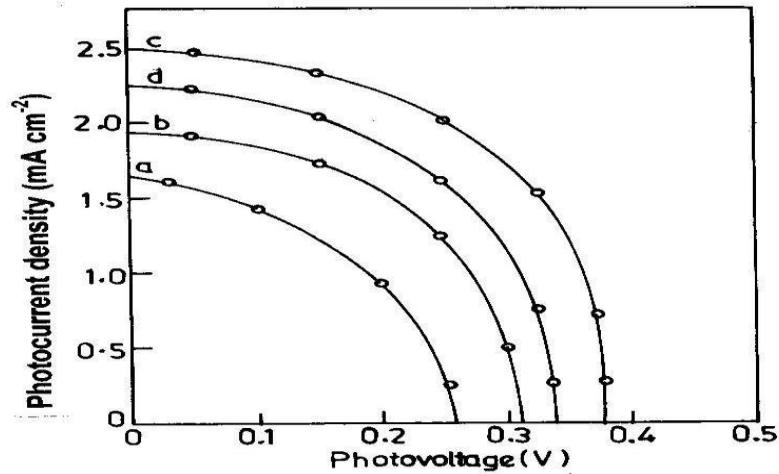


Fig: 12. – Load characteristics of In_2S_3 films deposited at 33 % duty cycles and post heat treated at different temperatures (a) 400°C (b) 450°C (c) 500°C and (d) 525°C

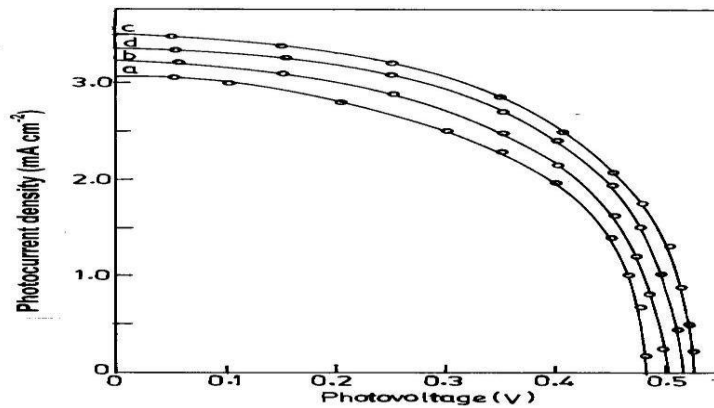


Fig: 13. – Load characteristics of In_2S_3 films deposited at 50 % duty cycles and post heat treated at different temperatures (a) 400°C (b) 450°C (c) 500°C and (d) 525°C

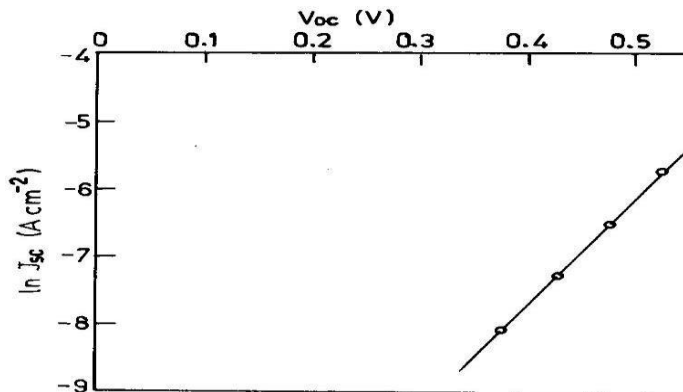


Fig: 14. – $\ln J_{sc}$ Vs V_{oc} plot for In_2S_3 films deposited at 50 % duty cycle

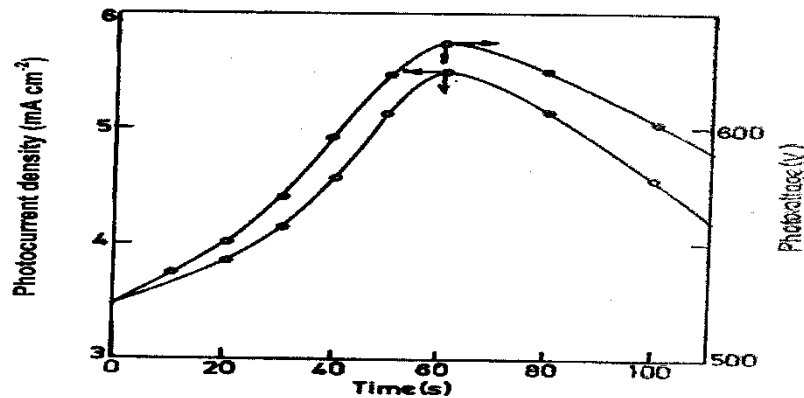


Fig: 15. – Variation of Photocurrent and photovoltage with photoetching time of 60 s, In_2S_3 photoelectrodes deposited at 50 % duty cycle and post heated at 500°C

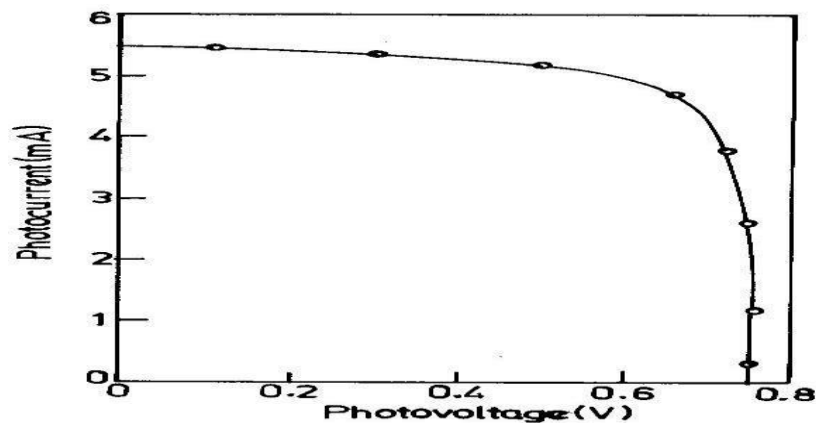


Fig: 16. – Load characteristics of In_2S_3 photoelectrodes deposited at 50 % duty cycle and post heat treated at 500°C after photoetching for 60s.

Table: 2. Photovoltaic parameters of In_2S_3 films deposited at different duty cycles and post heat treated at 500°C (Int : 60 mW cm^{-2})

Duty cycle (%)	V_{oc} (V)	J_{sc} (mA cm^{-2})	ff	η (%)	R_s (ohms)	R_{sh} (Kilo ohms)
6	0.33	1.80	0.59	0.58	17	2.6
9	0.35	2.00	0.64	0.75	14	2.6
15	0.40	2.12	0.55	0.77	12	2.5
33	0.40	2.50	0.56	0.89	9	2.6
50	0.43	4.50	0.53	1.71	6	2.5
50 (After Photograph)	0.48	5.80	0.68	3.13	4	2.6

Mott-Schottky plots ($1/C^2$ vs V) were studied using $1\text{M Na}_2\text{SO}_4$ as the blocking electrolyte and a EG&G PARC impedance analyzer model 6310. The In_2S_3 films heat treated at different temperatures were used as working electrode, graphite was used as counter electrode and SCE was used as the reference electrode. The frequency was fixed at 1 KHz and the bias voltage



was varied in the range -0.8 to $+0.4$ V vs SCE, the value of C was estimated from the imaginary part of the impedance using the equation,

$$C = 1 / 2\pi fZ$$

Fig: 17 exhibits the Mott-Schottky plots for the films heat treated at different temperatures in the range $450 - 550^\circ\text{C}$. The nature of the plot indicates n-type behavior. Extrapolation of the plot to the voltage axis yields a V_{fb} in the range of -0.74 V (SCE) to -0.76 V (SCE). The value of carrier density from the slope of the plot yields a value around $3.5 \times 10^{17} \text{ cm}^{-3}$. This value agrees well with the carrier density obtained from Hall measurements.

Spectral response measurements were carried out on the photoelectrodes by using photophysics monochromator and a 250W tungsten halogen lamp, 1M polysulphide as electrolyte, graphite as counter electrode and the photoelectrode as the working electrode. The wavelength was varied in the range $300 - 900$ nm and the photocurrent (J_{ph}) were noted at each wavelength. Plot of J_{ph} vs λ for the In_2S_3 electrode heat treated at 500°C is shown in Fig: 18. The value of $J_{ph(\text{max})}$ occurs at $0.86 \mu\text{m}$ corresponding to the band gap of 2.04 eV. This value matches well with the band gap value of 2.04 eV estimated from optical absorption measurements.

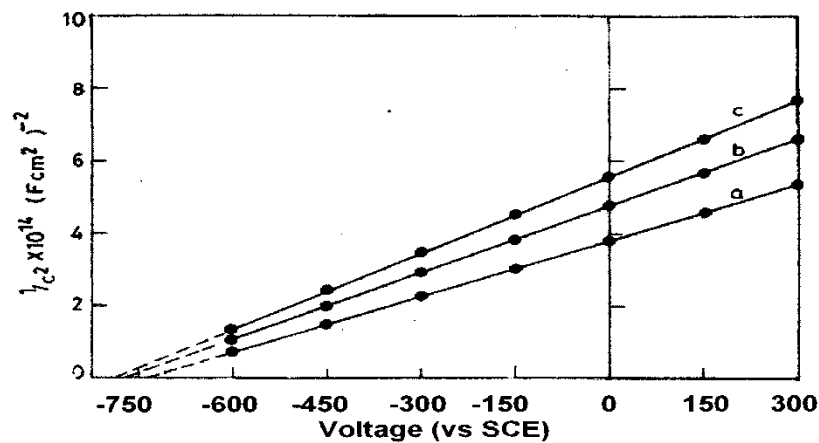


Fig: 17. – Mott Schottky plots of In_2S_3 electrodes annealed in argon at different temperatures (a) 450°C (b) 500°C (c) 550°C

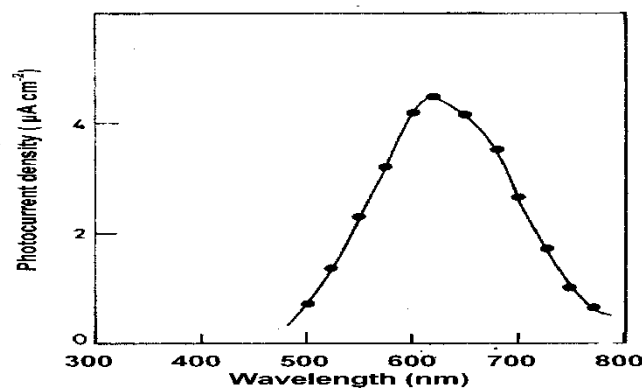


Fig: 18. – Variation of J_{ph} vs wavelength for In_2S_3 electrodes annealed in argon at 500°C

Conclusion

The In_2S_3 films have been deposited by the pulse plating technique at different substrate temperatures. The influences of pulse electroplating parameters like the substrate temperature on the film growth, structural, optical, electrical and photoelectrical properties have been studied.



XRD data was in the range of 50-90 nm with increase of duty cycle. The strain and dislocation density of the In_2S_3 films was found to be increased as the duty cycle increases. EDAX studies of In_2S_3 indicating the presence of In and S. The XPS analysis exhibits the binding energies of the $\text{In}3d$ and $\text{S}2p$. The Mott-Schottky plots of In_2S_3 films indicated n type behavior with a flat band potential of the order of 0.74 V (SCE). The band gap value of 2.04 eV estimated from optical absorption measurements.

References

1. R. Diehl, R. Nitsche, J. Cryst. Growth 28 (1975) 306.
2. S. Yu, L. Shu, Y. Qian, Y. Xie, J. Yang, L. Yang, Mater. Res. Bull. 33 (1998) 717.
3. E. Dalas, L. Kobotiatis, J. Mater. Sci. 28 (1993) 6595.
4. R.S. Mane, C.D. Lokhande, Mater. Chem. Phys.78 (2002) 15.
5. R. Kumaresan, M. Ichimura, N. Stato, P. Ramasamy, Mat.Sci.Engg.B: solid State 9 (2002) 37
6. W. Kim, C. Kim, J.Appl.Phys, 60(1986)2631.
7. M. Mathew, R. Jayakrishnan, P.M.R. Kumar, C.S. Kartha, K.P. Vijayakumar, Y. Kashiwaba, T. Abe, J. Appl. Phys. 100 (2006) 33504.
8. J.P. Mangalhar, R. Thangaraj and O.P. Agnihotri, Bull. Mater.Sci.,10(1988)333.
9. C. Guillén and J. Herrero, Thin Solid Films 510 (2006) 260.
10. J. Alvarez-Garcia, A. Perez-Rodriguez, A. Romano-Rodriguez, T. Jawhari, J.R. Morante, R. Scheer, W. Calvet, Thin Solid Films 387 (2001) 216.